Muon-spin-rotation measurements of the penetration depth in Li_2Pd_3B

R. Khasanov,[1,2] I. L. Landau,[3] C. Baines,[2] F. La Mattina,[1] A. Maisuradze,[1] K. Togano,[4] and H. Keller[1]
[1]*Physik-Institut der Universität Zürich, Winterthurerstrasse 190, CH-8057 Zürich, Switzerland*
[2]*Laboratory for Muon Spin Spectroscopy, Paul Scherrer Institute, CH-5232 Villigen PSI, Switzerland*
[3]*Kapitza Institute for Physical Problems, 117334 Moscow, Russia*
[4]*National Institute for Materials Science 1-2-1, Sengen, Tsukuba, Ibaraki 305-0047, Japan*
(Received 9 January 2006; published 29 June 2006)

Measurements of the magnetic field penetration depth λ in the ternary boride superconductor Li_2Pd_3B ($T_c \simeq 7.3$ K) have been carried out by means of muon-spin rotation (μSR). The absolute values of λ, the Ginzburg-Landau parameter κ, and the first H_{c1} and second H_{c2} critical fields at $T=0$ obtained from μSR were found to be $\lambda(0)=252(2)$ nm, $\kappa(0)=27(1)$, $\mu_0 H_{c1}(0)=9.5(1)$ mT, and $\mu_0 H_{c2}(0)=3.66(8)$ T, respectively. The zero-temperature value of the superconducting gap $\Delta_0=1.31(3)$ meV was found, corresponding to the ratio $2\Delta_0/k_B T_c=4.0(1)$. At low temperatures $\lambda(T)$ saturates and becomes constant below $T\simeq 0.2T_c$, in agreement with what is expected for s-wave BCS superconductors. Our results suggest that Li_2Pd_3B is a s-wave BCS superconductor with only one isotropic energy gap.

DOI: 10.1103/PhysRevB.73.214528 PACS number(s): 74.70.Ad, 74.25.Op, 74.25.Ha, 76.75.+i

I. INTRODUCTION

The discovery of superconductivity in the ternary boride superconductors Li_2Pd_3B and Li_2Pt_3B has attracted considerable interest in the study of these materials.[1–6] It is believed now that superconductivity in both the above-mentioned compounds is most likely mediated by phonons. It stems from photoemission,[3] nuclear magnetic resonance (NMR),[4] and specific heat experiments.[6] Moreover, the observation of a Hebel-Slichter peak in the ^{11}B spin-lattice relaxation rate in Li_2Pd_3B strongly supports singlet pairing.[4] However, experimental results concerning the structure of the superconducting energy gap are still controversal. On the one hand, NMR data of Li_2Pd_3B (Ref. 4) and specific heat data of Li_2Pd_3B and Li_2Pt_3B (Ref. 6) can be well explained assuming conventional superconductivity. On the other hand, recent measurements of the magnetic field penetration depth λ suggest unconventional behavior of both compounds, namely, double-gap superconductivity in Li_3Pd_2B and nodes in the energy gap in Li_3Pt_2B.[5,7] This contradiction is serious and shows that further experimental investigations of these compounds are needed.

In this paper, we report a systematic study of magnetic field penetration depth λ in Li_2Pd_3B by means of transverse-field muon-spin rotation (TF-μSR) (the detailed description of the TF-μSR technique in connection with λ studies can be found, e.g., in Ref. 8). Measurements were performed down to 30 mK in a series of fields ranging from 0.02 to 2.3 T. For all magnetic fields studied (0.02, 0.1, 0.5, 1, and 2.3 T) no sign of a second superconducting gap was detected. All our results may be well explained by assuming conventional superconductivity with only *one isotropic* energy gap. The absolute values of λ, the Ginzburg-Landau parameter κ, and the first (H_{c1}) and second (H_{c2}) critical fields at $T=0$ obtained from μSR were found to be $\lambda(0)=252(2)$ nm, $\kappa(0)=27(1)$, $\mu_0 H_{c1}(0)=9.5(1)$ mT, and $\mu_0 H_{c2}(0)=3.66(8)$ T, respectively. The zero temperature value of the superconducting gap Δ_0 was found to be 1.31(3) meV that corresponds to the ratio $2\Delta_0/k_B T_c=4.0(1)$.

The paper is organized as follows: In Sec. II we describe the sample preparation procedure and the TF-μSR technique in connection with $\lambda(T)$ measurements. In Sec. III A we discuss the temperature dependence of the second critical field H_{c2}. In Sec. III B we present the calculation of the absolute value of λ and the magnetic field dependence of the second moment of the μSR line. Section III C comprises studies of the temperature dependence of λ. The conclusions follow in Sec. IV.

II. EXPERIMENTAL DETAILS

The Li_2Pd_3B polycrystalline sample was prepared by two-step arc melting.[1] First, a binary Pd_3B alloy was prepared by conventional arc melting from the mixture of Pd(99.9%) and B(99.5%). The alloying of Li was done in the second arc melting, in which a small piece of Pd_3B alloy was placed on a Li(>99%) plate. Once the Pd_3B alloy melted, the reaction with Li occurred and developed very fast, forming a small button specimen (around 300 mg). Since the loss of Li was inevitable, the Li concentration in the final sample was estimated from the weight change. The deviation of the Li concentration from the stoichiometric one was less than 1% for the specimens used in this experiment.

Field-cooled magnetization (M_{FC}) measurements were performed with a superconducting quantum interference device (SQUID) magnetometer in fields ranging from 0.5 mT to 4 T and temperatures between 1.75 and 10 K. The $M_{FC}(T)$ curve for $\mu_0 H=0.5$ mT is shown in Fig. 1. The superconducting transition is rather broad indicating that the sample is not particularly uniform, i.e., the superconducting transition temperature may be evaluated only approximately. The middle point of the transition corresponds to $T_c^{(mp)}=7.1$ K, while the linear extrapolation of the steepest part of the $M(T)$ curve to $M=0$ results in $T_c^{(ext)}=7.6$ K (see Fig. 1).

TF-μSR experiments were performed at the πM3 beam line at the Paul Scherrer Institute (Villigen, Switzerland). The Li_2Pd_3B sample was field cooled from above T_c down to

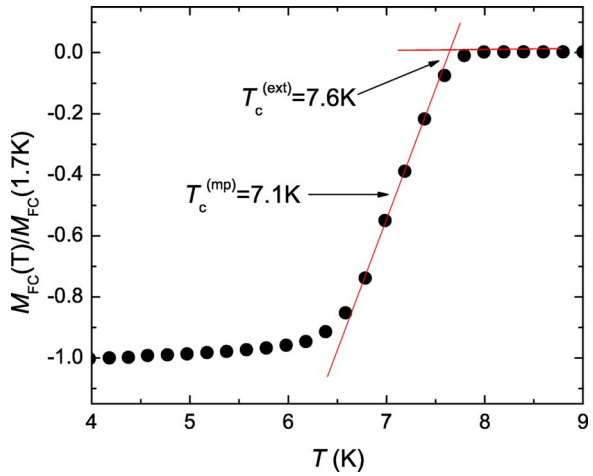

FIG. 1. (Color online) The normalized field-cooled magnetization curve $[M_{FC}(T)/M_{FC}(1.7\ \mathrm{K})]$ for $\mu_0 H=0.5$ mT. The solid line is the best linear fit to the steepest part of the $M_{FC}(T)$ curve. $T_c^{(mp)}$ and $T_c^{(ext)}$ are indicated in the figure and discussed in the text.

30 mK in fields of 2.3, 1, and 0.5 T, and down to $\simeq$1.6 K in fields of 0.1 and 0.02 T. In the transverse-field geometry the local magnetic field distribution $P(B)$ inside the superconducting sample in the mixed state, probed by means of the TF-μSR technique, is determined by the values of the coherence length ξ and the magnetic field penetration depth λ. In extreme type-II superconductors ($\lambda \gg \xi$) the $P(B)$ distribution is almost independent on ξ and the second moment of $P(B)$ line becomes simply proportional to $1/\lambda^4$.[9,10]

The μSR signal was recorded in the usual time-differential way by counting positrons from decaying muons as a function of time. The time dependence of the positron rate is given by the expression[11]

$$N(t) = N_0 \frac{1}{\tau_\mu} e^{-t/\tau_\mu}[1 + aP(t)] + bg, \tag{1}$$

where N_0 is the normalization constant, bg denotes the time-independent background, $\tau_\mu = 2.19703(4) \times 10^{-6}$ s is the muon lifetime, a is the maximum decay asymmetry for the particular detector telescope ($a \sim 0.18$ in our case), and $P(t)$ is the polarization of the muon ensemble

$$P(t) = \int P(B)\cos(\gamma_\mu B t + \phi) dB. \tag{2}$$

Here $\gamma_\mu = 2\pi \times 135.5342$ MHz/T is the muon gyromagnetic ratio and ϕ is the angle between the initial muon polarization and the effective symmetry axis of a positron detector. $P(t)$ can be linked to the internal field distribution $P(B)$ by using the algorithm of Fourier transform.[11]

The $P(t)$ and $P(B)$ distributions inside the Li_2Pd_3B sample in the normal (T=8.5 K) and in the mixed state (T =2 K) after field cooling in a magnetic field of 0.1 T are shown in Fig. 2. The $P(B)$ distributions were obtained from the measured $P(t)$ by using the fast Fourier transform procedure based on the maximum entropy algorithm.[12] In the normal state, a symmetric line at the position of the external

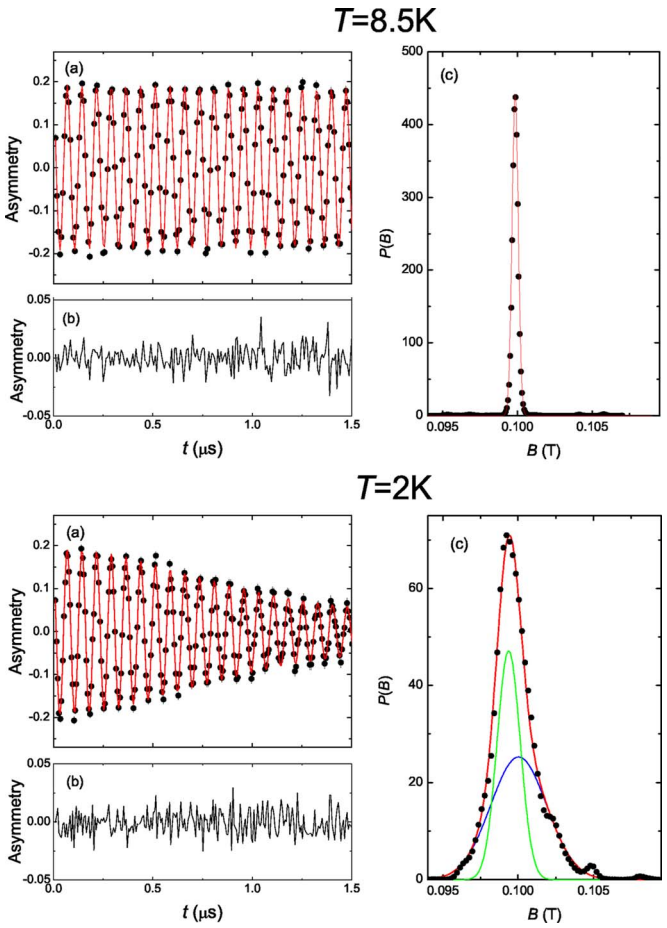

FIG. 2. (Color online) μSR time spectra and magnetic field distributions of Li_2Pd_3B taken above (T=8.5 K) and below (T =2 K) the superconducting transition temperature T_c in $\mu_0 H$ =0.1 T: (a) the muon-time spectra, (b) difference between the one Gaussian (upper panel) and two Gaussian (lower panel) fits and experimental data, (c) internal field distributions inside the Li_2Pd_3B sample. The lines represent the best fit with the Gaussian line shapes. See text for details.

magnetic field with a broadening arising from the nuclear magnetic moments is seen. Below T_c the field distribution is broadened and asymmetric. In order to account for the asymmetric field distribution, μSR time spectra obtained below T_c were fitted by two Gaussian lines[13,14]

$$P(t) = \sum_{i=1}^{2} A_i \exp(-\sigma_i^2 t^2/2)\cos(\gamma_\mu B_i t + \phi), \tag{3}$$

where A_i, σ_i, and B_i are the asymmetry, the Gaussian relaxation rate, and the first moment of the i-th line, respectively. At $T > T_c$, the analysis is simplified to a single line with $\sigma_{nm} \sim 0.1$ MHz arising from the nuclear moments of the sample. Equation (3) is equivalent to the field distribution[14]

$$P(B) = \gamma_\mu \sum_{i=1}^{2} \frac{A_i}{\sigma_i} \exp\left(-\frac{\gamma_\mu^2 (B - B_i)^2}{2\sigma_i^2}\right). \tag{4}$$

The solid lines in Figs. 2(a) represent the best fit with the one (upper panel) and two Gaussian lines (lower panel) to the

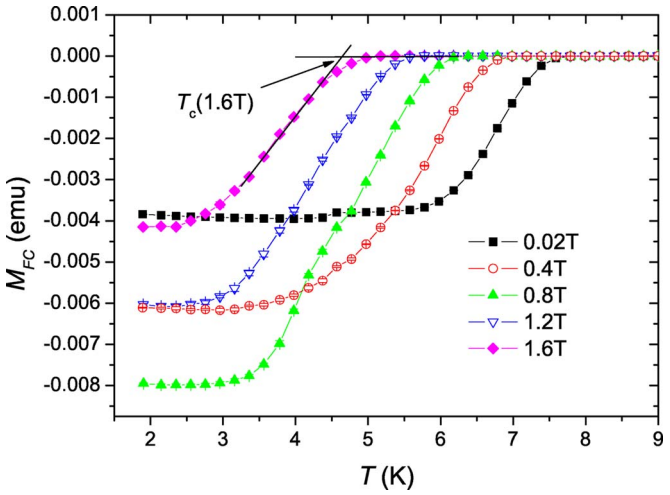

FIG. 3. (Color online) Field-cooled magnetization curves $M_{FC}(T)$ of Li_2Pd_3B taken at various magnetic fields: from the left to the right $\mu_0 H = 1.6$, 1.2, 0.8, 0.4, and 0.02 T. The paramagnetic background was subtracted.

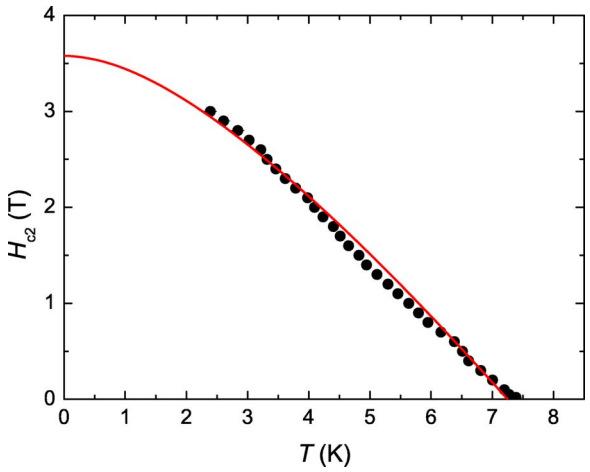

FIG. 4. (Color online) Temperature dependence of the upper critical field H_{c2} of Li_2Pd_3B. The solid line is the fit using the WHH model. The fit parameters are listed in the text.

μSR time spectra. The corresponding $P(B)$ lines are shown in Figs. 2(c). For this distribution the mean field and the second moment are[14]

$$\langle B \rangle = \sum_{i=1}^{2} \frac{A_i B_i}{A_1 + A_2} \tag{5}$$

and

$$\langle \Delta B^2 \rangle = \frac{\sigma^2}{\gamma_\mu^2} = \sum_{i=1}^{2} \frac{A_i}{A_1 + A_2} \left[\frac{\sigma_i^2}{\gamma_\mu^2} + [B_i - \langle B \rangle]^2 \right]. \tag{6}$$

The superconducting part of the square root of the second moment σ_{sc} was then obtained by subtracting the contribution of nuclear moments σ_{nm} measured at $T > T_c$ as $\sigma_{sc}^2 = \sigma^2 - \sigma_{nm}^2$. From the known value of σ_{sc} the absolute value of λ can be evaluated using the following relation:

$$\sigma_{sc}[\mu s^{-1}] = 4.83 \times 10^4 (1 - H/H_{c2})[1 + 1.21(1 - \sqrt{H/H_{c2}})^3] \lambda^{-2}[\text{nm}], \tag{7}$$

which describes the field variation of σ_{sc} for an ideal triangular vortex lattice.[10] Note, that according to Ref. 10, Eq. (7) does not hold for very low magnetic inductions.

III. EXPERIMENTAL RESULTS AND DISCUSSION

A. Temperature dependence of the upper critical field

The field-cooled magnetization $M_{FC}(T)$ curves for several magnetic fields H are shown in Fig. 3. For each particular field H the corresponding transition temperature $T_c(H)$ was taken as an intersect of the linear extrapolation of the steepest part of the $M_{FC}(H)$ curve with $M = 0$ line. The resulting $H_{c2}(T)$ dependence is presented in Fig. 4. It is seen that $H_{c2}(T)$ data can be satisfactorily fitted with the model provided by the Werthamer-Helfand-Hohenberg (WHH) theory.[15] The fit yields $H_{c2}(0) = 3.58(10)$ T and $T_c = 7.25$ K. Note, that the value of the transition temperature obtained from the fit lies between $T_c^{(mp)}$ and $T_c^{(ext)}$ introduced in Fig. 1, i.e., it is in agreement with low-field magnetization measurements. In the following, the $H_{c2}(T)$ curve presented in Fig. 4 is used to analyze the μSR data (see Sec. III C).

To summarize, the temperature dependence of the second critical field can be well described within the WHH theory. The absolute value of the second critical field at $T = 0$ was found to be 3.58(10) T in agreement with results of Badica *et al.*[2]

B. Magnetic field dependence of the second moment of μSR line

In Fig. 5(a) the temperature dependences of σ_{sc} for $\mu_0 H = 0.02$, 0.1, 0.5, 1, and 2.3 T are shown. For $\mu_0 H = 0.5$, 1, and 2.3 T, $\sigma_{sc}(T)$ was measured down to 30 mK. It is seen, that below 1.5 K σ_{sc} is practically temperature independent [Fig. 5(b)]. Bearing in mind that the temperature dependence of σ_{sc} saturates at low temperatures, the values of $\sigma_{sc}(T = 0)$ can be reliably evaluated for all magnetic fields. The results are plotted in Fig. 6 as a function of H. For $\mu_0 H = 0.5$, 1.0, and 2.3 T $\sigma_{sc}(0)$ was obtained from the zero slope linear fit of the $T \leq 1.5$ K data [see Fig. 5(b)] and for $\mu_0 H = 0.02$ and 0.1 T $\sigma_{sc}(0)$ was assumed to be equal to σ_{sc} at the lowest measured temperature ($T \simeq 1.55$ K). The solid line in Fig. 6 represents the result of the fit of Eq. (7) to the experimental data with $H_{c2}(0) = 3.66(8)$ T and $\lambda(0) = 252(2)$ nm. As it was already mentioned above, Eq. (7) does not hold for very low magnetic fields. For this reason the data point for $\mu_0 H = 0.02$ T was excluded from the fit. It is seen (Fig. 6), that the theoretical curve perfectly matches all data points for $\mu_0 H \geq 0.1$ T. The value of σ_{sc} for $\mu_0 H = 0.02$ T lies slightly below the theoretical curve, as expected. It is important to emphasize that the value of $\mu_0 H_{c2}(0) = 3.66(8)$ T obtained from the fit of $\sigma_{sc}(0, H)$ data coincides within the error with $\mu_0 H_{c2}(0) = 3.58(10)$ T, evaluated in the previous section from the directly measured $H_{c2}(T)$. This good agreement between the values of H_{c2}, obtained from the two completely

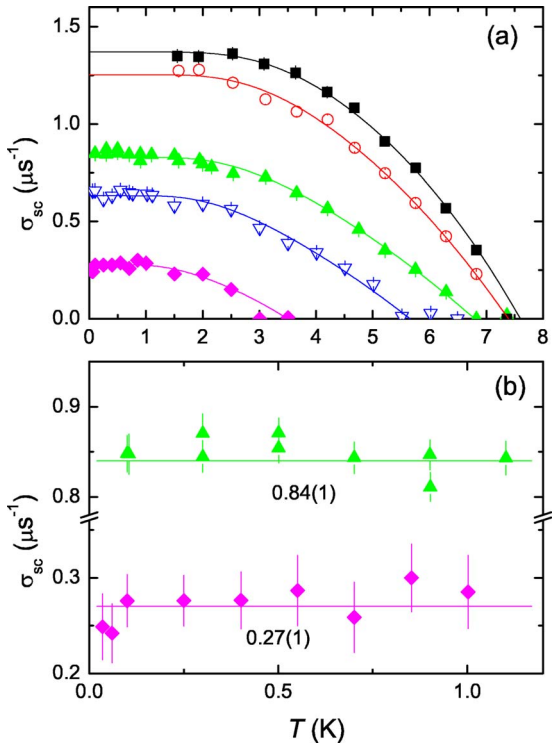

FIG. 5. (Color online) (a) Temperature dependencies of σ_{sc} measured in various magnetic fields (from top to the bottom) 0.02, 0.1, 0.5, 1, and 2.3 T. The solid lines are guides to the eye. (b) Low-temperature part of $\sigma_{sc}(T)$ for $H=0.5$ and 2.3 T.

different experiments, demonstrates the validity of our analysis.

The above-presented experiments show unambiguously that λ, evaluated from μSR measurements, is *magnetic field independent*, as one would expect in case of a conventional superconductor with isotropic energy gap.[16] On the other hand, in superconductors with nodes in the gap and isotropic double-gap superconductors like MgB_2, λ, evaluated in the same way, increases with increasing magnetic field (see, e.g., Refs. 13, 16, and 17). Thus, the fact, that the $\sigma_{sc}(0)$ versus H dependence is perfectly described by the field independent λ (see Fig. 6), implies that Li_2Pd_3B is a *conventional single-gap* superconductor.

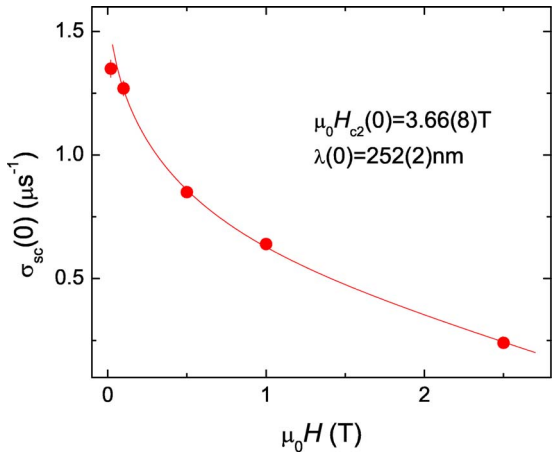

FIG. 6. (Color online) Field dependence of the zero-temperature μSR depolarization rate $\sigma_{sc}(0)$ in the Li_2Pd_3B sample. The solid line corresponds to a fit of Eq. (7) to the experimental data with the parameters given in the text.

The zero-temperature value of the superconducting coherence length $\xi(0)$ may be estimated from $H_{c2}(0)$ as $\xi(0)=[\Phi_0/2\pi H_{c2}(0)]^{0.5}$, which results in $\xi(0)=9.5(2)$ nm (Φ_0 is the magnetic flux quantum). Using the values of $\lambda(0)$ and $\xi(0)$, one can evaluate the zero-temperature value of the Ginzburg-Landau parameter $\kappa(0)=\lambda(0)/\xi(0)\approx 27(1)$. The value of the first critical field can be calculated by means of Eq. (4) from Ref. 10 as $\mu_0 H_{c1}=9.5(1)$ mT. It is remarkable that all superconducting characteristics of Li_2Pd_3B could be obtained solely from μSR experiments.

To summarize, the magnetic field dependence of the superconducting part of the μSR depolarization rate σ_{sc} is well described within the Ginzburg-Landau theory for anisotropic single-gap superconductors. The zero-temperature values of the first and second critical fields, the magnetic penetration depth, the coherence length, and the Ginzburg-Landau parameter were found to be $\mu_0 H_{c2}(0)=3.66(8)$ T, $\mu_0 H_{c1}=9.5(1)$ mT, $\lambda(0)=252(2)$ nm, $\xi(0)=9.5(2)$ nm, and $\kappa=27(1)$, respectively.

C. Temperature dependence of λ

Equation (7) implies that σ_{sc} depends on λ and the reduced magnetic field H/H_{c2}. It is also clear that σ_{sc} vanishes for $H \geq H_{c2}(T)$. This means that in order to obtain the temperature dependence of λ from the $\sigma_{sc}(T)$ curves, the temperature dependence of H/H_{c2} must be taken into account. In our calculations, the $H_{c2}(T)$ curve provided by the solid line in Fig. 4 was used. Due to the known value of $\kappa=27(1)$, we are not limited by Eq. (7) but can directly apply the numerical calculations of Brandt.[10] In this case, the results collected in the lowest magnetic field ($\mu_0 H=0.02$ T) can also be used. The resulting temperature dependence of λ is shown in Fig. 7. Remarkably, all λ points, reconstructed from σ_{sc} measured in various magnetic fields, collapse onto a single $\lambda(T)$ curve. It should be emphasized that in this reconstruction no adjustable parameter was used. The $\sigma_{sc}(T)$ dependences were obtained by means of μSR, while the $H_{c2}(T)$ curve was measured in a completely different set of magnetization experiments (see Sec. III A).

Considering the temperature dependence of λ, one should note that it can be better described by the BCS theory for a moderate coupling with the zero-temperature energy gap $2\Delta_0=4.0(1)k_BT_c$ [$\Delta(0)=1.31(3)$ meV] rather than for the weak coupling limit. This is in agreement with the value $2\Delta_0=3.94k_BT_c$ obtained recently from specific-heat measurements.[6] The upward deviations of the experimental data points from the theoretical curve at higher temperatures (see Fig. 7) is expected for nonuniform samples (e.g., for the samples where the transition temperatures are distributed via a certain range ΔT_c). At temperatures close to T_c $\lambda^{-2} \sim (T_c - T)$. Assuming that the critical temperature varies throughout the sample from $T_{c0}-\Delta T_c$ to T_{c0}, then the relative variation of λ^{-2} for $T < T_{c0}-\Delta T_c$ is proportional to $[1-\Delta T_c/(T_{c0}$

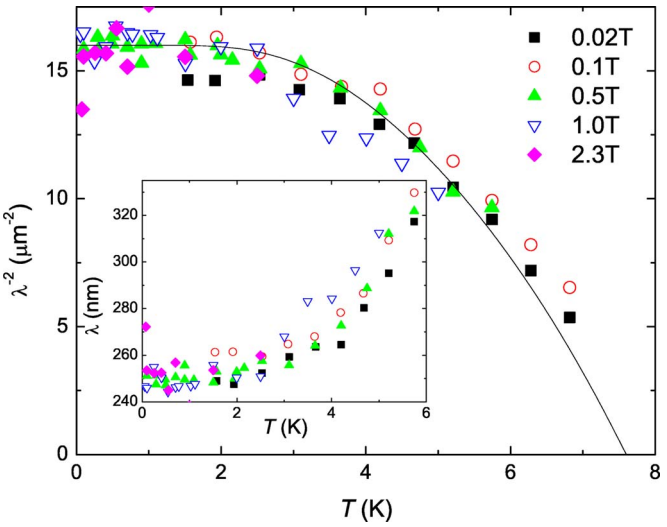

FIG. 7. (Color online) $1/\lambda^2$ *versus* temperature. The solid line represents the theoretical curve provided by the BCS theory for $2\Delta_0=4k_BT_c$ with $T_c=T_c^{\text{ext}}=7.6$ K (see Fig. 1). The inset shows $\lambda(T)$. The errors are not shown for clarity.

$-T)]^{-1}$, i.e., it increases with increasing temperature. The value of σ, resulting from μSR experiments in the case of nonuniform samples, may be written as $\sigma^2=1/V_0\int\sigma_{\text{local}}^2dV$ (σ_{local} is the local value of σ in the unit volume dV and V_0 is the sample volume). Taking into account that $\sigma_{\text{local}}^2 \sim 1/\lambda_{\text{local}}^4$ this averaging implies that the parts of the sample with the smallest values of λ (the highest values of T_c) provide the main contribution to σ_{sc}. At lower temperatures, however, λ become more uniform throughout the sample and σ_{sc} can be used for reliable calculations of $\lambda(T)$.

Recently, Yuan *et al.* studied the magnetic field penetration depth in Li_2Pd_3B by means of self-inductance technique.[5,7] It was obtained that a considerable increase of λ starts already at temperatures well below 1 K. Since such a behavior contradicts conventional BCS theory, the authors assumed the presence of the second superconducting gap. Our results (see Fig. 7) are quite different. $\lambda(T)$, evaluated from μSR measurements, is practically temperature independent below 2 K in complete agreement with conventional single-gap theories of superconductivity. We argue that the most probable reason for the above-mentioned disagreement in the $\lambda(T)$ dependence comes from the difference in the experimental techniques. The self-inductance technique used in Refs. 5 and 7 provides information about the properties of the surface of the sample. It is likely that in this Li-containing compound the properties of the surface layer of the sample are different from those of the bulk.

To summarize, in the whole temperature range (from T_c down to 30 mK) the temperature dependence of λ is consistent with what is expected for a single-gap s-wave BCS superconductor. The value of the superconducting gap was found to be $\Delta_0=1.31(3)$ meV, that corresponds to the ratio $2\Delta_0/k_BT_c=4.0(1)$.

IV. CONCLUSIONS

Muon-spin rotation and magnetization studies were performed on the ternary boride superconductor Li_2Pd_3B ($T_c \simeq 7.3$ K). The main results are (i) The absolute values of λ, ξ, κ, H_{c1}, and H_{c2} at zero temperature obtained from μSR are $\lambda(0)=252(2)$ nm, $\xi(0)=9.5$ nm, $\kappa(0)=27(1)$, $\mu_0H_{c1}(0)=9.5(1)$ mT, and $\mu_0H_{c2}(0)=3.66(8)$ T. (ii) The values of $H_{c2}(0)$ evaluated from μSR and magnetization measurements coincide within the experimental accuracy. (iii) Over the whole temperature range (from T_c down to 30 mK) the temperature dependence of λ is consistent with what is expected for a single-gap s-wave BCS superconductor. (iv) No influence of the applied magnetic field to $\lambda(T)$ was observed. (v) At $T=0$, the magnetic field dependence of σ_{sc} is in agreement with what is expected for a superconductor with an isotropic energy gap.

To conclude, all the above-mentioned features suggest that Li_2Pd_3B is a *BCS superconductor with an isotropic energy gap*.

ACKNOWLEDGMENTS

This work was partly performed at the Swiss Muon Source (SμS), Paul Scherrer Institute (PSI, Switzerland). The authors are grateful to S. Strässle for help during manuscript preparation. This work was supported by the Swiss National Science Foundation, in part by the NCCR program MaNEP, and the K. Alex Müller Foundation.

[1] K. Togano, P. Badica, Y. Nakamori, S. Orimo, H. Takeya, and K. Hirata, Phys. Rev. Lett. **93**, 247004 (2004).
[2] P. Badica, T. Kondo, T. Kudo, Y. Nakamori, S. Orimo, and K. Togano, Appl. Phys. Lett. **85**, 4433 (2004).
[3] T. Yokoya, T. Muro, I. Hase, H. Takeya, K. Hirata, and K. Togano, Phys. Rev. B **71**, 092507 (2005).
[4] M. Nishiyama, Y. Inada, and Guo-qing Zheng, Phys. Rev. B **71**, 220505(R) (2005).
[5] H. Q. Yuan, D. Vandervelde, M. B. Salamon, P. Badica, and K. Togano, cond-mat/0506771 (unpublished).
[6] H. Takeya, K. Hirata, K. Yamaura, K. Togano, M. El Massalami, R. Rapp, F. A. Chaves, and B. Ouladdiaf, Phys. Rev. B **72**, 104506 (2005).
[7] H. Q. Yuan, D. F. Agterberg, N. Hayashi, P. Badica, D. Vandervelde, K. Togano, M. Sigrist, and M. B. Salamon, cond-mat/0512601 (unpublished).
[8] P. Zimmermann, H. Keller, S. L. Lee, I. M. Savic, M. Warden, D. Zech, R. Cubitt, E. M. Forgan, E. Kaldis, J. Karpinski, and C. Krüger, Phys. Rev. B **52**, 541 (1995).
[9] E. H. Brandt, Phys. Rev. B **37**, 2349 (1988).
[10] E. H. Brandt, Phys. Rev. B **68**, 054506 (2003).
[11] A. Schenck, *Muon Spin Rotation: Principles and Applications in Solid State Physics* (Adam Hilger, Bristol, 1986); S. F. J. Cox, J. Phys. C **20**, 3187 (1987); J. H. Brewer, "Muon Spin Rotation/Relaxation/Resonance" in *Encyclopedia of Applied Physics*, Vol. 11, p. 23 (VCH, New York, 1995).
[12] B. D. Rainford and G. J. Daniell, Hyperfine Interact. **87**, 1129 (1994).

[13] S. Serventi, G. Allodi, R. De Renzi, G. Guidi, L. Romano, P. Manfrinetti, A. Palenzona, Ch. Niedermayer, A. Amato, and Ch. Baines, Phys. Rev. Lett. **93**, 217003 (2004).

[14] R. Khasanov, D. G. Eshchenko, D. Di Castro, A. Shengelaya, F. La Mattina, A. Maisuradze, C. Baines, H. Luetkens, J. Karpinski, S. M. Kazakov, and H. Keller, Phys. Rev. B **72**, 104504 (2005).

[15] E. Helfand and N. R. Werthamer, Phys. Rev. **147**, 288 (1966); N. R. Werthamer, E. Helfand, and P. C. Hohenberg, *ibid.* **147**, 295 (1966).

[16] R. Kadono, J. Phys.: Condens. Matter **16**, S4421 (2004).

[17] J. Sonier, J. Brewer, and R. Kiefl, Rev. Mod. Phys. **72**, 769 (2000).